

Rapid and effective synthesis of $^{40}\text{Ca}^+ - ^{27}\text{Al}^+$ ion pair towards quantum logic optical clock

Junjuan Shang¹²³, Kaifeng Cui¹²³, Jian Cao¹², Shaomao Wang¹²³, Hualin Shu¹², Xueren Huang¹² *

¹ State Key Laboratory of Magnetic Resonance and Atomic and Molecular Physics, Wuhan Institute of Physics and Mathematics, Chinese Academy of Sciences, Wuhan 430071

² Key Laboratory of Atom Frequency Standards, Wuhan Institute of Physics and Mathematics

³ University of Chinese Academy of Sciences, Beijing 100049, China

Received: date / Revised version: date

Abstract High precision atomic clocks have been applied not only to very important technological problems such as synchronization and global navigation systems, but to the fundamental precision measurement physics. Single $^{27}\text{Al}^+$ is one of the most attractions of selection system due to its very low blackbody radiation effect which dominates frequency shifts in other optical clock systems. Up to now, the $^{27}\text{Al}^+$ still could not be laser-cooled directly by reason that the absence of 167nm laser. Sympathetic cooling is a viable method to solve this problem. In this work, we used a single laser cooled $^{40}\text{Ca}^+$ to sympathetically cool one $^{27}\text{Al}^+$ in linear Paul trap. Comparing to laser ablation method we got a much lower initial energy (0.63eV) atoms sprayed from a home-made atom oven, which would make loading aluminum ion more efficient and the sympathetic cooling much easier. The probability of loading single $^{27}\text{Al}^+$ is about 80%. By precisely measuring the secular frequency of the ion pair, finally the dark ion species, $^{27}\text{Al}^+$, was proved, which could be used to quantum logic optical frequency standard.

207 851(6) Hz [11], which means $^{27}\text{Al}^+$ has a higher stability at the same feedback velocity compared to other ions, such as $^{40}\text{Ca}^+$, $^{171}\text{Yb}^+$ and so on. Both the $^1\text{S}_0$ and $^3\text{P}_0$ energy levels exhibit only a weak dependence on the magnetic fields for the Zeeman effect with angular momentum $J=0$ [12]. As well as it is insensitive to electric field gradients. Moreover, blackbody radiation shift of this transition is $8(3)\text{E-18}$ at room temperature [13]. However, since it is not easy to acquire the direct cooling laser (167nm), $^{27}\text{Al}^+$ is performed sympathetic cooling with a simultaneously trapped ion and readout spectrum with quantum logic spectrum (QLS) [11, 14]. $^{40}\text{Ca}^+$ is one of the popular ion species in optical standard and quantum information processing (QIP). The lasers applied to $^{40}\text{Ca}^+$ can be acquired from external cavity diode laser, which is simpler and stability. We choose $^{40}\text{Ca}^+$ as our frozen species.

Sympathetic cooling system includes target and frozen species which are interacting with each other. The temperatures of these two species are very low because frozen species can be laser cooled to low temperature and target species interact or collide with frozen species to transfer energy with them. Effectiveness of sympathetic cooling is with strong dependence on the initial energy [15]. sympathetic cooling is one significant technique in quantum information processing (QIP) [16], cold molecules [17], optical frequency standard [1, 18] and chemical reactions at very low temperatures [19].

1 Introduction

Single atomic ions trapped in an RF Paul trap [1–5] and atomic ensemble trapped in an optical lattice [6–8] are the most two primary approaches of optical clock experiments. It has been demonstrated that optical clock frequency measurement had a fractional uncertainty of 10^{-18} in systems based on $^{27}\text{Al}^+$, $^{171}\text{Yb}^+$, ^{88}Sr and ^{171}Yb atoms respectively. The $^{27}\text{Al}^+$ clock based on the $^1\text{S}_0 - ^3\text{P}_0$ transition is stable enough as a reference for an optical clock [9, 10]. The natural linewidth of $^3\text{P}_0$ state is 8mHz and the measured transition frequency is 1121 015 393

Here, using a new design of atom oven could generate low velocity, the $^{40}\text{Ca}^+ - ^{27}\text{Al}^+$ ion pair was synthesized rapidly and effectively. The mean time of sympathetic cooling by $^{40}\text{Ca}^+$ was about 330s, as the low initial energy made it easy to be trapped and cooled. The secular motion frequency ratio of $^{40}\text{Ca}^+ - ^{27}\text{Al}^+$ ion pair and $^{40}\text{Ca}^+$ has been measured in our trap, which fitted well with theoretical calculation.

* hxueren@wipm.ac.cn

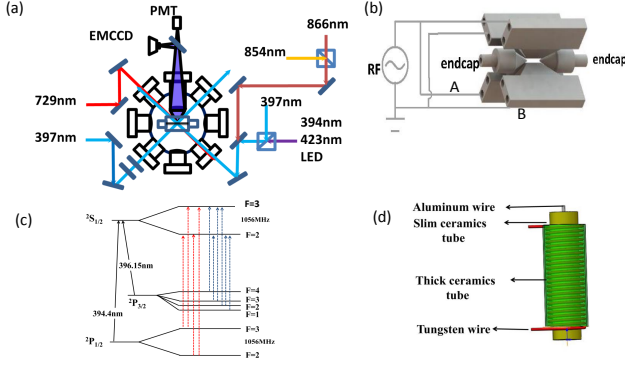


Fig. 1 (a) and (b) is Experimental setup and ion trap. (c) and (d) is the Aluminum atom energy and Aluminum oven setup.

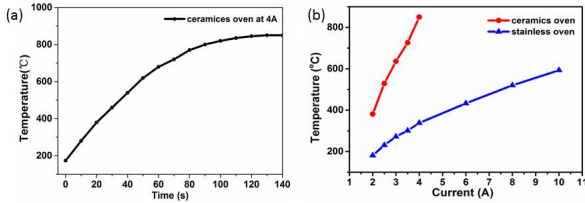


Fig. 2 The relation of the temperature of oven with (a) time at 4A current and (b) heating current.

2 Experimental apparatus

The experiment setup is shown in Fig.???. A linear Paul trap was made of stainless steel with a dimension of $2r_0=1.6\text{mm}$ and $2z_0=5\text{mm}$ to confine ions. A radiofrequency (RF) voltage at the frequency 17.128 MHz was applied to blade-like electrodes A and the other pair blade-like electrodes B were RF grounded. The endcap electrodes were with DC voltage (Fig.??(b)). ^{40}Ca oven and ^{27}Al oven were placed under the electric shield stage with an angle of 25° angle to prevent calcium or aluminum atom from adhering to the electrodes which may cause the electric field of ion trap change. The ion trap was enclosed in a UHV chamber ($3\text{E}-8\text{Pa}$) evacuated by a 75L/s ion pump (Fig.??(a)). The external-cavity diode laser of 423nm and LED of 395nm were used to photo-ionization of ^{40}Ca , moreover the 394nm laser served as ^{27}Al photo-ionization laser. The $^{40}\text{Ca}^+$ was Doppler cooled by 397nm and 866nm lasers. The $^{40}\text{Ca}^+$ fluorescence was detected by PMT and EMCCD. Fig.??(c) shows the energy level of ^{27}Al .

We designed 20mm length stainless steel tube oven with diameter 1.5mm, and thickness 0.1mm to generate ^{40}Ca and ^{27}Al atoms. In experiment only ^{40}Ca atom signal was detected. The relation between temperature and the current applied to oven have been measured with

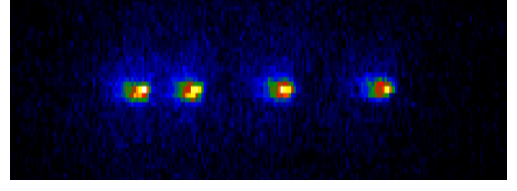


Fig. 3 6 ions of $^{40}\text{Ca}^+$ and $^{27}\text{Al}^+$ mixture ion crystal

thermos couple in vacuum chamber (0.1Pa). The temperature of stainless steel tube oven is only 600°C at 11A current. Since the saturated vapor pressure of ^{27}Al is very low, the ^{27}Al must be heated high than 700°C the atom signal could be detected. For above reason a ceramics tube oven was designed to supersede the traditional stainless oven. The oven included two ceramic tubes and tungsten wire. One ceramics tube was spiral wound with tungsten wire. And both embedded in another ceramics tube (Fig. 1(b)). The temperature of new oven was also measured and the result was displayed in Fig. 2. Temperature of ceramics oven is obvious high compared to stainless steel oven at the same current and the time of heating to 700°C is about 2 minutes.

3 Experimental results

$^{40}\text{Ca}^+ (^{27}\text{Al}^+)$ was generated by photo ionization neutral calcium (aluminum) atom beam, which could reduce the impaction of stray electric field. The specific number of ions were obtained by controlling the time of heating calcium (aluminum) oven at about 300°C (700°C). After several minutes later the ions was loaded in the ion trap one by one. It was necessary to block the photo-ionization laser after loading ions because the oven was still with high temperature after shutting down the current.

After $^{40}\text{Ca}^+$ was trapped in the ion trap, the current was applied to the aluminum oven and illuminated 394nm laser with $500\mu\text{W}$ power to insert $^{27}\text{Al}^+$ to the $^{40}\text{Ca}^+$ chain. The RF power and endcap voltage must be reduced because the temperature of ions was high at the same time when $^{27}\text{Al}^+$ generated. Several minutes later the position of $^{40}\text{Ca}^+$ in the CCD shifted which indicated that dark ion was trapped. The number of dark ions could be diagnosed by ions distance because the distances of neighboring ions is related to the number of ions, it has no relation with ion species as long as they are singly charged. And the ions hopped back and forth between different axial positions when low DC voltages applied to the endcaps. The different positions of $^{40}\text{Ca}^+$ were imaged with CCD, as shown in Fig. 3. By adding several of such images together, it could be showing the ions at all different positions. And then the dark ions number is confirmed.

Sympathetic cooling process as a sequence of successive Coulomb collisions between the particles transfers

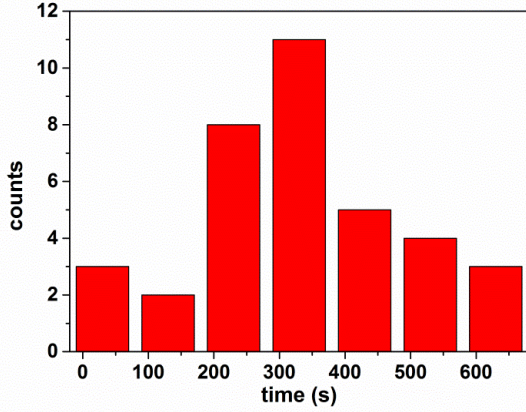


Fig. 4 Distribution of cooling times, measured by recording the time it takes a laser cooled $^{40}\text{Ca}^+$ ion to crystallize a hot $^{27}\text{Al}^+$ ion. The histogram shows that the cooling may vary by an order of magnitude

momentum from the target ion to the frozen ion held at low temperature by laser cooling. The time ($\tau_{cooling}$) needed from cooling ion cloud to crystal state is [15]:

$$\tau_{cooling} = \frac{8\pi^3 \epsilon_0^2}{3e^4} \times \frac{E_0^2 m_f}{\omega^3 m_i^2} \quad (1)$$

where E_0 and ω are the initial energy of target ion and the oscillating frequency. The m_f and m_i correspond to the mass of frozen and target ion. The $\tau_{cooling}$ is with strong dependence on the initial energy. The statistics of $\tau_{cooling}$ from 36 numbers of evens is shown in Fig. 3. Recording the time from heating oven to $^{27}\text{Al}^+$ crystal and then subtracting the time of loading hot $^{27}\text{Al}^+$, the cooling time was obtained. Mostly, the cooling time was about 330s corresponding to the initial energy was 0.63eV according to Fig. 4 which was lower than that of $^{27}\text{Al}^+$ generated by laser ablation (600s) [15]. Furthermore, the target ion with high initial energy may kick out the frozen ion. In our experiments, it is 80% probability to loading single $^{27}\text{Al}^+$.

The dark ions might be some ions other than $^{27}\text{Al}^+$ because $^{40}\text{Ca}^+$ and $^{27}\text{Al}^+$ can react with background gas to molecular ions, such as CaH^+ , AlH^+ [20,21] and so on. In addition, there are no differences in the CCD image. Thus the mass of dark ions should be measured to know the ions species. To diagnose of the dark ions, we measured the frequency of vibrational modes of two mixed ion species. The mode frequency of the ions along axial direction depends on the mass as well as the arrangement of the ions, and can be calculated numerically [8], the secular motion frequency for two ions is

$$\omega'_z = \sqrt{\frac{1 + \mu - \sqrt{1 - \mu + \mu^2}}{\mu}} \omega_z \quad (2)$$

where ω and μ is the secular motion frequency of single ion and the mass ratio, respectively. For $^{40}\text{Ca}^+ - ^{27}\text{Al}^+$

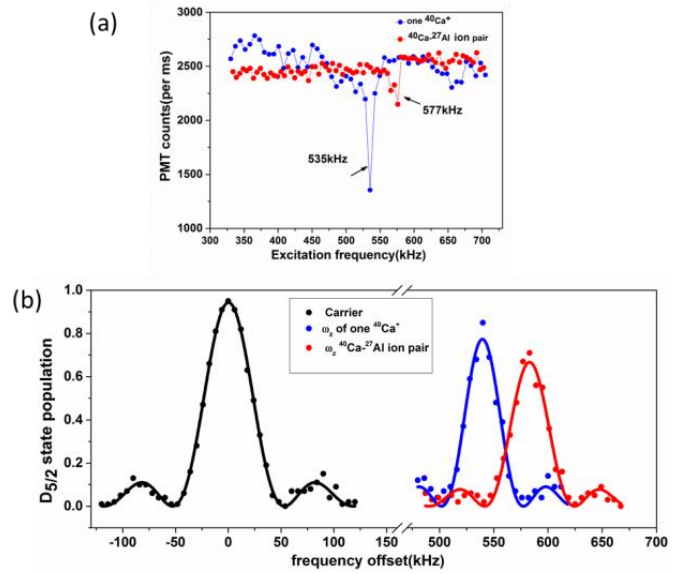


Fig. 5 Measurement the ω_z using (a) RF resonance and (b) secular motion sideband spectrum

ion pair the common frequencies are calculated as 1.083 relative to that of two $^{40}\text{Ca}^+$ center-of-mass mode. The secular motion frequency can be measured by RF resonance [22] and $^{40}\text{Ca}^+$ ions secular motion sideband spectra [23].

The secular motion excitation mass spectrum along z axial can be measured by applying the characteristic perturbation RF voltages to one of the endcaps. When the frequency is resonant with the secular motion frequency, the ion starts to oscillate along the excited normal mode direction. Then, its amplitude of motion could be determined by the electric field. And the laser-induced fluorescence (LIF) counts decreases or increases due to the changing Doppler width of the cooling transition. The mass spectrum could be measured precisely using secular motion sideband spectra. The secular motion sideband spectrum is different when have or not dark ion. Fig. 5 displays the measurement results by above two methods. Fig. 5(a) shows PMT counts against with the RF frequency. The blue line gives the motion resonant spectrums of one $^{40}\text{Ca}^+$ and the red one is the case of $^{40}\text{Ca}^+ - ^{27}\text{Al}^+$ pair. The ω_z are 535 kHz and 577 kHz respectively. And Fig. 5(b) is the carrier and secular sideband spectrum. The secular sideband spectrum of $^{40}\text{Ca}^+ - ^{27}\text{Al}^+$ ion pair was shifted about 40 kHz comparing with single $^{40}\text{Ca}^+$. We could get the ratio of secular motion frequency 1.078 ± 0.012 and 1.086 ± 0.02 which fits well with theoretical calculation. That meant the ion pair obtained was $^{40}\text{Ca}^+ - ^{27}\text{Al}^+$ ion pair.

4 Conclusions

In this report, $^{40}\text{Ca}^+ - ^{27}\text{Al}^+$ ion pair was synthesized rapidly and effectively by using a novel oven heating. The

average time of sympathetic cooling was about 330s. In addition, the new designed oven can also be used to heat other materials evaporated under high temperature. The drawback of new design oven is that it is possible to load more than one $^{27}\text{Al}^+$ due to unable block the aluminum atom beam immediately. The dark ion mass was distinguished by the ion mass spectrum which was measured and analyzed by using RF resonance and secular motion sideband spectra. The rapid and effective synthesis of $^{40}\text{Ca}^+ \cdot ^{27}\text{Al}^+$ ion pair is significance and necessary on progress of $^{27}\text{Al}^+$ quantum logic optical clock in the near future.

Acknowledgements We thank for Songbai Kang for the early works, thank P. O. Schmidt, Ting Chen and Yao Huang for discuss. This work was supported by Ministry of Science and Technology of the People,s Republic of China under project of 2012AA120701.

References

1. C. W. Chou, D. B. Hume, J. C. J. Koelemeij, D. J. Wineland, T. Rosenband, Phys. Rev. Lett. 104, 070802 (2010)
2. P. Dube, A. A. Madej, A. Shiner, B. Jian, Phys. Rev. A 92,042119 (2015).
3. R. M. Godun, P. B. R. Nisbet-Jones, J. M. Jones, S. A. King, L. A. M. Johnson, H. S. Margolis, K. Szymaniec, S. N. Lea, K. Bongs, P. Gill, Phys. Rev. Lett. 113,210801 (2014).
4. Y. Huang, H.Guan, P. Liu, W. Bian, L. Ma, K. Liang, T. Li, K. Gao, Phys. Rev. Lett. 116, 013001 (2012).
5. T. Rosenband, D. B. Hume, P. O. Schmidt, C. W. Chou, A. Brusch, L. Lorini, W. H. Oskay, R. E. Drullinger, T. M. Fortier, J. E. Stalnaker, S. A. Diddams, W. C. Swann, N. R. Newbury, W. M. Itano, D. J. Wineland, J. C. Bergquist, Science, 319, 1808 (2008).
6. T. L. Nicholson, S. L. Campbell, R. B. Hutson, G. E. Marti, B. J. Bloom, R. L. McNally, W. Zhang, M. D. Barrett, M. S. Safronova, G. F. Strouse, W. L. Tew, J. Ye, Nat.Comm. 6,6896 (2015).
7. N. Hinkley, J. A. Sherman, N. B. Phillips, M. Schioppo, N. D. Lemke, K. Beloy, M. Pizzocaro, C. W. Oates, A. D. Ludlow, Science, 341, 6151 (2013).
8. J. J. McFerran, L. Yi, S. Mejri, W. Zhang, S. Di Manno, M. Abgrall, J. Guena, Y. Le Coq, S. Bize, Phys. Rev. A 89,050501 (2014).
9. H. G. Dehmelt, IEEE Trans. Instrum. Meas. 31, 83 (1982).
10. N. Yu, H. Dehmelt, W. Nagourney, Proc. Natl. Acad. SciUSA. 89,7289 (1992).
11. T. Rosenband, P. O. Schmidt, D. B. Hume, W. M. Itano, T. M. Fortier, J. E. Stalnaker, K. Kim, S. A. Diddams, J. C. J. Koelemeij, J. C. Bergquist, D. J. Wineland, Phys. Rev. Lett. 98, 220801 (2007).
12. D. B. Hume, thesis, 1, (2010).
13. W. M. I. T. Rosenband, P. O. Schmidt, D. B. Hume, arXiv:phscis, 0611125v2, (2006).
14. P. O. Schmidt, T. Rosenband, C. Langer, W. Itano, J. Bergquist, D. Wineland, Science, 309, 5735 (2005).
15. M. Guggemos, D. Heinrich, O. Herrera-Sancho, R. Blatt, C. Roos, New J. Phys. 17, 103001 (2015).
16. H. Rohde, S. T. Gulde, C. F. Roos, P. A. Barton, D. Leibfried, J. Eschner, F. Schmidt-Kaler, R. Blatt, J. Opt. B:Quantum Semiclassical Opt. 3, S34 (2001).
17. N. Kimura, K. Okada, T. Takayanagi, M. Wada, S. Ohtani, H. A. Schuessler, Phys. Rev. A 83,053413 (2011).
18. K. Hayasaka, Appl. Phys. B 107,965 (2012).
19. K. Okada, M. Wada, L. Boesten, T. Nakamura, I. Katayama, S. Ohtani, J. of Phys. B 36, 33 (2003).
20. W. M. Macalpine, R. O. Schildknecht, Proc. of the IRE. 47, 2099 (1959).
21. N. B. Khanyile, G. Shu, K. R. Brown, Nat. Commun. 6,7825 (2015).
22. D. Wineland, H. Dehmelt, Int. J. Mass Spectrom. Ion Phys. 16, 338 (1975).
23. H. Dehmelt, Bull Am. Phys. Soc. 20, 60 (1975).